

Background charge noise in metallic single-electron tunneling devices

A. B. Zorin, F.-J. Ahlers, J. Niemeyer, T. Weimann, and H. Wolf
Physikalisch-Technische Bundesanstalt, D-38116 Braunschweig, Germany

V. A. Krupenin and S. V. Lotkhov
Laboratory of Cryoelectronics, Moscow State University, 119899 Moscow, Russia
 (Received 11 October 1995)

With the help of two single-electron tunneling transistors whose islands were positioned about 100 nm apart, a low-frequency charge noise generated in the Al_2O_3 substrate has been measured. The signals detected by these electrometers have shown a 10–20 % correlation in power in the 1–10-Hz range. Using a simple model we show that the charge noise sources (fluctuating traps) can be distributed either in thin dielectric layers (including the barriers) adjacent to the islands or, alternatively but more likely, in a volume of the substrate. [S0163-1829(96)07420-6]

I. INTRODUCTION

In the last decade, the technology of fabrication of the metallic single-electron tunneling (SET) circuits has made great progress.¹ Due to a reduction of the geometrical sizes of the structures designed, the capacitances of tunnel junctions and metallic islands can be reliably realized on the subfemtofarad level. This ensures that the characteristic Coulomb energy E_C by far exceeds the energy of thermal fluctuations $k_B T$ for a typical dilution refrigerator temperature. However, numerous experiments have shown that the performance of SET devices strongly suffers from background charge fluctuations (see, for example, Chaps. 3, 7, and 9 of Ref. 1 and references therein). At low frequencies, they substantially dominate over intrinsic fluctuations in devices, which are mainly due to shot noise. The deep understanding of the nature of background charge noise and the search for ways to reduce it are, therefore, very important for practical SET devices.

Present-day knowledge of the background charges, which was accumulated essentially in experiments with SET transistors (electrometers), is limited by the following facts. First, the charge fluctuations are significant at low frequencies and they usually have a $1/f$ spectrum with a roll-off frequency of 100–1000 Hz. With some exceptions, the intensity is in the range of 10^{-3} – $10^{-4} e/\sqrt{\text{Hz}}$ at $f=10$ Hz (Refs. 2–8) and nearly temperature independent at $T \leq 300$ mK.⁸ Second, some samples clearly produce a telegraph noise with random switching between 2, 3, or more states with a magnitude of up to $0.1e$.^{3–5,7} Third, for some substrate materials (e.g., SiO_2 and Al_2O_3), the nonzero background charge and, to some extent, its fluctuations can decay with a long time constant^{2,9} (hours and even days) if a sample remains at low temperature and a fixed small bias. Thermal cycling or application of large drain and/or gate voltages immediately activates the noise again. Mechanical stress⁹ or a weak surface electroacoustic wave in the piezoelectric substrate¹⁰ (GaAs) acts in the same direction. Fourth, the intensity of detected noise seems to be correlated with the design of the island and the gate electrodes,^{5,6} and it has

been noticed that smaller islands normally produce less noise.⁷

Relying on these experimental facts there is the belief that in general the background charge noise is due to the activity of random traps for single electrons in dielectric materials surrounding an island. These traps have different switching times and trapping energies and hence they can generate low-frequency noise.¹¹ Specifically, in the case of noninteracting traps with a uniform distribution of trapping energies, the spectrum becomes $1/f$ -like.¹² Thus, a $1/f$ spectrum or a spectrum close to it points to numerous traps participating in the generation of noise. As regards a probable location of traps, opinions are divided. For example, Song *et al.*⁸ suggest that noise originated from junction barriers dominates in the total charge noise. Their argumentation is based on the fact that an electric field produced by the charged island is mainly concentrated inside the oxide layer of the tunnel junction, and for that reason the motion of a charge in that region produces a larger polarization of the island in accordance with Green's reciprocity theorem. On the other hand, Zimmerli *et al.*⁴ consider that fluctuating traps located in a dielectric substrate might contribute essentially to total noise. In the following, we present the results of experiments that show that noise coming from the substrate is comparable with or probably larger than that from the barriers, at least for the sample under consideration.

II. THE EXPERIMENT

The basic idea of our experiment stems from the fact that two individually biased SET electrometers, whose islands are placed on the same substrate close to each other, can detect similar noise signals coming from the traps located in that substrate. As opposed to this, the noise signals that are due to switching of the traps inside tunnel barriers are obviously noncorrelated because a charge in the barrier is screened by the junction electrodes. The origin of the noise can, therefore, be determined using dual channel spectrum analysis. Such analysis could be perfect if the space diagrams for the sensitivity of two electrometers were similar and capacitive coupling between the islands leading to cross-talk

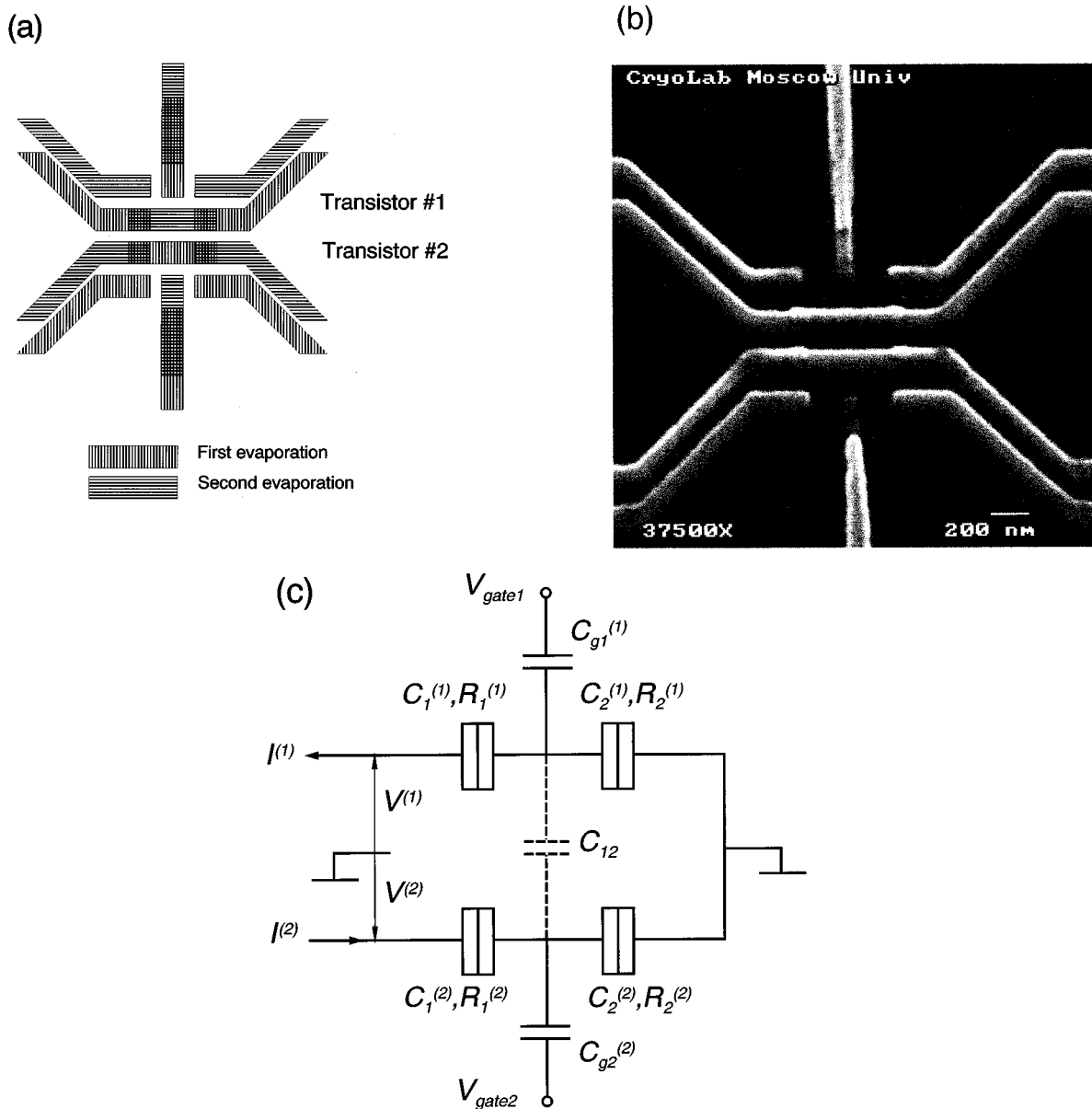


FIG. 1. (a) A schematic drawing of the resulting Al layers after two evaporations through the suspended mask, (b) a SEM picture of the structure, and (c) the circuit diagram.

between two transistors was small. Although these two requirements are in conflict with each other, they can be approximately fulfilled in practice.

A. Technique

The sample was fabricated on a Si chip coated by a sputtered Al_2O_3 layer 200 nm thick. The Al- AlO_x -Al tunnel junctions were made using standard two-angle shadow evaporation through a suspended mask. We used electron beam lithography for patterning fine lines in a three-layer polymethylmethacrylate (PMMA)/Ge/copolymer mask, which was then developed in 10% solution of isopropanol. The Ge layer was etched in CF_4 plasma and then the pattern was transferred to the copolymer by oxygen plasma. To reduce the mechanical stress in the three layer system, a new vacuum low-temperature (100 °C) soft baking technique was applied for e -beam-sensitive PMMA heat treatment before

exposure.¹³ The UV light exposure procedure was applied to fabricate the ‘‘coarse’’ pattern (with sizes larger than 10 μm). Two evaporations of Al and an oxidation in between were made *in situ*. Tilting of the substrate between two depositions was made in the plane perpendicular to the axes of the in-line structures of each transistor. As a result of the first evaporation (25 nm thick), the outer leads of transistor 1 and the island of transistor 2 were produced, while in the second evaporation (35 nm thick) the island of transistor 1 and the outer leads of transistor 2 completed the whole device [see Fig. 1(a)]. Each island has its ‘‘own’’ gate electrode represented by a straight strip (evaporated twice) situated perpendicular to the transistor axis. The resulting twin-transistor structure has a minimum number of stray shadow lines [see the SEM picture in Fig. 1(b)]. The islands have lateral dimensions of approximately $600 \times 100 \text{ nm}^2$ and are 100 nm apart.

The measurements were made in a dilution refrigerator at a temperature of 30 mK. The normal state of Al was maintained by applying a magnetic field of 1 T. The transistors, as is shown in the electric circuit diagram of Fig. 1(c), were biased by dc currents $I^{(1,2)}$ from individual sources and the voltages $V^{(1,2)}$ were picked up in the bandwidth from 0 to 300 Hz. Besides the low-pass filters each biasing and signal line was supplied by a 1-m-long section of Thermocoax[®] cable, which was at the temperature of the mixing chamber throughout most of its length.¹⁴ The room-temperature electronics was placed inside an rf shielded cabin. The equivalent voltage noise of the setup referred to an amplifier input was determined for a cold load resistor and amounted to ≤ 30 nV/ $\sqrt{\text{Hz}}$ at 10 Hz. An HP 89410A dual channel spectrum analyzer was used for the noise measurements.

B. Results

From the measured I - V characteristics we deduced the asymptotic normal-state resistances of each electrometer, which turned out to be $R_{\Sigma}^{(1)} \equiv R_1^{(1)} + R_2^{(1)} \approx 141$ k Ω and $R_{\Sigma}^{(2)} \equiv R_1^{(2)} + R_2^{(2)} \approx 126$ k Ω . From the offset voltages $V_{\text{off}}^{(1,2)} = e/C_{\Sigma}^{(1,2)}$ (see, e.g., Chap. 2 in Ref. 1), we found the island capacitances $C_{\Sigma}^{(1)} \approx C_{\Sigma}^{(2)} \approx 0.49$ fF, where

$$C_{\Sigma}^{(1,2)} \approx C_1^{(1,2)} + C_2^{(1,2)} + C_{g1,2}^{(1,2)} + C_{12}, \quad (1)$$

and the corresponding Coulomb energy $E_C^{(1,2)} = e^2/2C_{\Sigma}^{(1,2)} \approx 160$ $\mu\text{eV} \approx k_B \times 1.85$ K. The V versus V_{gate} characteristics shown in Fig. 2 indicated good symmetry of the junction capacitances $C_1^{(1,2)} \approx C_2^{(1,2)} \approx 0.24$ fF and relative smallness of the gate capacitances $C_{g1}^{(1)} \approx 5.3$ aF and $C_{g2}^{(2)} \approx 5.6$ aF, which were derived from modulation periods $C_g \Delta V_{\text{gate}} = \Delta Q_0 \equiv e$, where Q_0 is the polarization charge of an island. The curves obtained by sweeping the voltage applied to the counter gates showed clearly smaller values of the corresponding capacitances $C_{g2}^{(1)} \approx 3.0$ aF and $C_{g1}^{(2)} \approx 2.8$ aF. The maximum values of the voltage-to-charge transfer coefficients defined by the maximum slopes of the modulation characteristics,

$$\begin{aligned} \eta^{(1,2)} &= |dV^{(1,2)}/dQ_0^{(1,2)}| \\ &\approx 0.5\text{--}0.6 \text{ mV}/e \text{ at } I^{(1,2)} \approx 0.2 \text{ nA}, \end{aligned} \quad (2)$$

were almost identical for both devices.

In order to evaluate the cross-talk due to capacitive coupling of the islands, we measured the capacitance $C_{12}^* \approx 13.2$ aF between island 2 and the whole body of transistor 1, where both outer electrodes and gate were connected and used as a new ‘‘gate.’’ As $C_{12}^* \ll C_{\Sigma}^{(1,2)}$, we obtained the upper estimate for the interisland mutual capacitance [shown in Fig. 1(c) by dashed lines] $C_{12} \leq C_{12}^*$ and, therefore, for the strength of the cross-talk

$$\kappa = C_{12}/C_{\Sigma}^{(1,2)} \leq C_{12}^*/C_{\Sigma}^{(1,2)} \approx 0.03. \quad (3)$$

This figure shows which part of the charge on one island is induced on the neighboring island. The possible electromagnetic coupling and hence the cross-talk between the signal wires inside the cryostat were negligibly small for all the frequencies of interest.

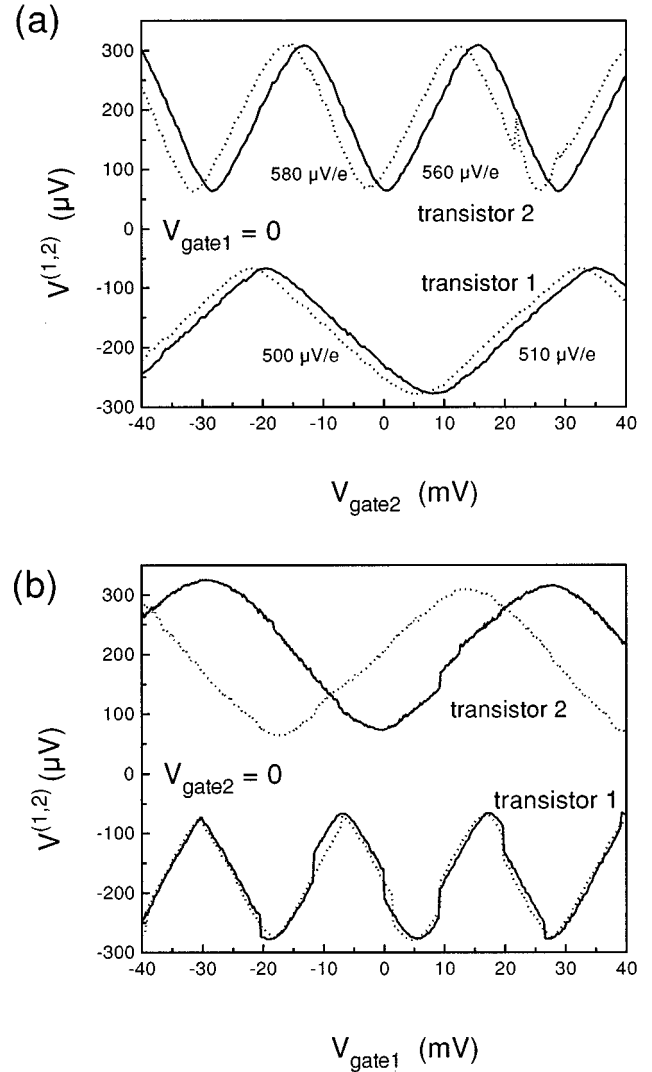


FIG. 2. The V vs V_{gate} modulation curves for (a) the second and (b) first gate sweeps recorded at bias currents $I^{(1)} = I^{(2)} = 0.2$ nA. The maximum values of response functions $\eta^{(1,2)}$ [Eq. (2)] are presented for both slopes in characteristics of each transistor in (a). Every pair of solid (dotted) curves was recorded one just after the other. The dotted series of curves were measured after a lapse of (a) 0.5 h and (b) 1 h.

Apart from the nicely uniform parameters, the sample was not free from ‘‘imperfections,’’ and this is clearly seen in Fig. 2(b). The sweeping of voltage applied to gate 1 almost always led to incremental jumps of a polarization charge $Q_0^{(1)}$. Among these jumps, those of approximately $0.1e$ (see the lower curves) dominated. In that case, electrometer 2 usually detected approximately 4.5 times smaller jumps of $Q_0^{(2)}$. Such behavior may be explained by incremental charging of a few impurities (traps) in the substrate, the ‘‘most active’’ of these being located closer to island 1 and/or its gate (1) than to island 2. We have recorded over 50 double signal traces at different rates of the gate voltage sweep, and the most typical curves are presented in Fig. 3. In order to increase the dynamic range in these measurements, the dc components were subtracted from the signals (the input filter time constant $\tau = 0.1$ s). As can be seen from the long-time scale records (a) and (c) in Fig. 3, the widths of noise traces

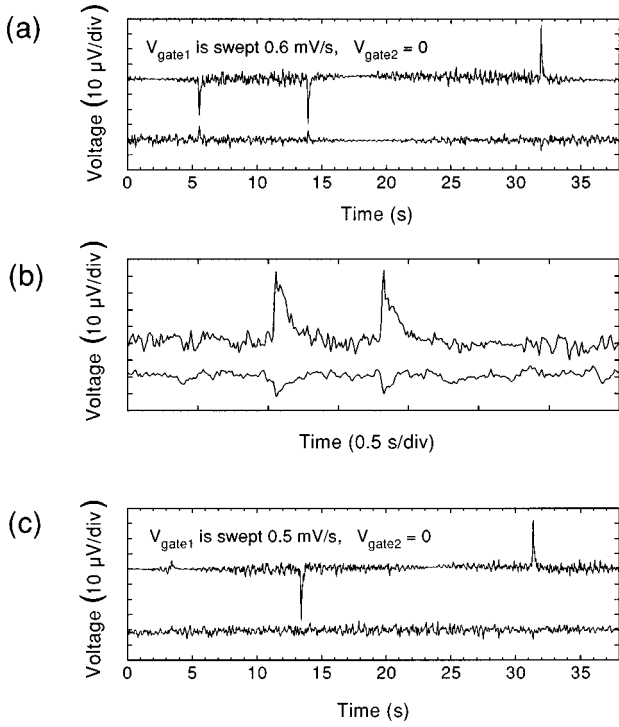


FIG. 3. Time traces of ac voltages on two transistors recorded when $V_{\text{gate}1}$ was swept. The curves are offset, so that the uppermost traces in all panels belong to transistor 1. The peaks are results of jumps of background charges and their signs together with the signs of $dV^{(1,2)}/dV_{\text{gate}1}$ determine the sign of the change of a charge.

are modulated, and this is in accordance with the dependence of the response coefficients $\eta^{(1,2)}$ on $Q_0^{(1,2)}(t)$. A clear correlation of the charge jump pulses in panels (a) and (b) can be seen. In particular, the fine time scale curves in (b) show the repeated incremental charging of the islands of both transistors when they reacted to obviously the same events that occurred one after another with a 0.78-s delay. On the other hand, very seldom the voltage spikes in the second channel were not noticeable [see the event that occurred at $t = 13.3$ s in (c)], pointing to a very weak correlation in these rare cases, if any.

The recorded traces characterize the noise in the case where a gate voltage is swept at a relatively high rate. Although this method clearly demonstrates the correlation, the sweeping electric field of the gate possibly enhances the natural charge noise in the substrate. Therefore, in order to characterize two noise signals and the correlation quantitatively, we adjusted and fixed the gate voltages in a way that provides a maximum for the two response coefficients $\eta^{(1)} \approx 510 \mu\text{V}/e$ and $\eta^{(2)} \approx 580 \mu\text{V}/e$. This maximum was attained at $V_{\text{gate}1} \approx 0$ and $V_{\text{gate}2} \approx 20$ mV [see Fig. 2(a)]. Then the power spectrum of signals in each channel was measured. Within the 10% margins, the measured noise power densities

$$S_{1,2}(\omega) \equiv \langle V_{\omega}^{(1,2)} V_{\omega}^{(1,2)*} \rangle \quad (4)$$

were equal in the range from 1 to 10 Hz, meaning that the input noise signals were also nearly equal because of almost similar parameters $\eta^{(1)} \approx \eta^{(2)}$. Therefore, instead of showing both quantities, S_1 and S_2 , we present in Fig. 4 their average

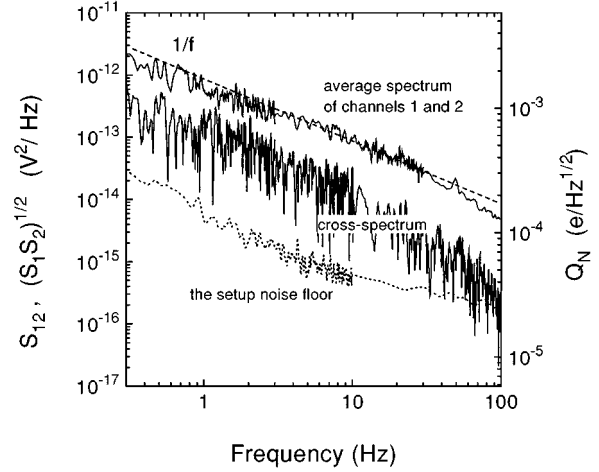


FIG. 4. The average spectrum density of channels 1 and 2 (in comparison with a $1/f$ dependence) and their cross spectrum. The right-hand axes translates the input noise into electron charge units. The dotted curve spectrum shows the noise power density in case of a cold resistor load.

value $(S_1 S_2)^{1/2}$ as a resulting noise figure. The corresponding rms voltage at 10 Hz was about $V_N \approx 300 \text{ nV}/\sqrt{\text{Hz}}$ which, in charge units, corresponds to the rather typical value of $Q_N = V_N / (\eta^{(1)} \eta^{(2)})^{1/2} \approx 5.5 \times 10^{-4} e/\sqrt{\text{Hz}}$.

In order to find correlation of two signals in the frequency domain, we measured the cross-spectrum power density (see, for example, Ref. 15)

$$S_{12}(\omega) \equiv \langle V_{\omega}^{(1)} V_{\omega}^{(2)*} \rangle. \quad (5)$$

Although the resulting curve (see Fig. 4) turned out to be rather noisy (the number of averagings performed, $N = 100$, was limited in time, to about 30 min, while the charge drift was small and the fixed gate voltages still provided the maximum values of $\eta^{(1,2)}$), it shows noticeable correlation of the fluctuation sources. According to our measurements, the dimensionless correlation factor is

$$\gamma \equiv |S_{12}| / (S_1 S_2)^{1/2} = 0.15 \pm 0.05 \quad (6)$$

in the frequency range from 1 to 10 Hz.

Taking into account that the space diagrams of sensitivity of two electrometers are obviously different, the result Eq. (6) definitely points to the fact that part (if not all) of the charge noise sources are located in the substrate. Note that the obtained value of γ is much higher than that one could expect in the case of the noise sources located only inside the tunnel junction barriers. Since the charges located in a thin barrier layer practically cause polarization of the neighboring island, the nonvanishing value of γ can be due only to electrostatic interaction of the islands, i.e., about $\kappa^2 \approx 10^{-3}$ [the squared ratio of polarization charges of two islands, see Eq. (3)]. Hence we conclude that the role of the substrate sources is substantial, and in order to quantify it, we propose the following simple model.

III. THE MODEL

Let us consider a system of two similar grounded conducting spheres of radius a [see Fig. 5(a)]. The spheres

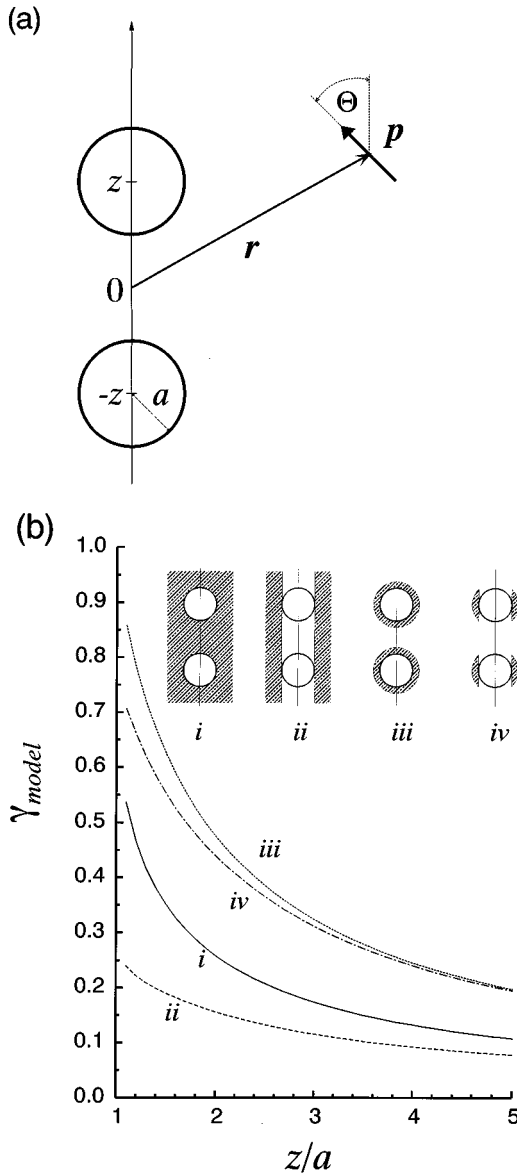


FIG. 5. (a) The model geometry and (b) the dependence of γ_{model} on the distance between two spherical islands calculated for different distribution of fluctuating sources in space. The inset shows these axially symmetric regions as shadowed areas; the thickness of the layers in (iii) and (iv) is equal to $0.1a$.

themselves model the bodies of islands, and grounding plays the role of tunnel junctions whose capacitances dominate in the total capacitances of the islands [Eq. (1)]. Since the dielectric permeability ε drops off in the final result, we consider it equal to unity assuming the vacuum medium. The two spheres' geometry makes possible an easy computation of the polarization of the islands caused by an arbitrarily positioned charge, without Poisson's equation having to be solved. It is based on the formula (see, for example, the textbook by Jackson¹⁶) giving the polarization of a single grounded sphere,

$$q_{\text{im}} = -(a/r)e, \quad \mathbf{r}_{\text{im}} = (a/r)^2 \mathbf{r}, \quad (7)$$

where q_{im} and \mathbf{r}_{im} are the magnitude and position of the image charge (inside a sphere), respectively, and $r = |\mathbf{r}| > a$ is

the distance between the initial charge e and the center of the sphere. For the case of two spheres, in accordance with the superposition principle, the polarization can be calculated by (infinite) summing up all image charges in each body appearing in the system of two "spherical mirrors." In practice, such a summing procedure rapidly converges, and this makes it convenient for a numerical calculation of the functions $q_{\text{im}}^{(1,2)}(\mathbf{r})$ describing polarization of each sphere by a single unit charge.

In order to model a fluctuating trap positioned in an arbitrary point of the outer space \mathbf{r} , let us assume that its switching is associated with a small displacement $\delta \mathbf{r}$ ($\delta r \ll a$) of the elementary charge e . This is equivalent to the creation (annihilation) of a dipole with the electric moment $\mathbf{p} = e \delta \mathbf{r}$ ($= -e \delta \mathbf{r}$), shown in Fig. 5(a), which induces on the spheres the polarization charges that are the functions of its position and orientation in space,

$$\delta Q^{(1,2)}(\mathbf{r}, \theta) = \nabla q_{\text{im}}^{(1,2)}(\mathbf{r}) \cdot \delta \mathbf{r}. \quad (8)$$

The corresponding contributions to the noise powers $\delta S_{1,2}$ and δS_{12} are proportional to the quantities $[\delta Q^{(1,2)}(\mathbf{r}, \theta)]^2$ and $[\delta Q^{(1)}(\mathbf{r}, \theta) \delta Q^{(2)}(\mathbf{r}, \theta)]$, respectively. Thus, for randomly orientated dipoles the total noise powers are expressed via the $\delta S_{1,2}$ and δS_{12} averaged over the angle $0 \leq \theta \leq \pi$; this averaging is performed explicitly. A uniform distribution of noninteracting fluctuators in the certain space region \mathcal{V} leads to spatial integration. Finally, for the correlation factor we have the ratio of the space-averaged quantities,

$$\gamma_{\text{model}} = \frac{\left| \int_{\mathcal{V}} d\mathbf{r} \nabla q_{\text{im}}^{(1)}(\mathbf{r}) \cdot \nabla q_{\text{im}}^{(2)}(\mathbf{r}) \right|}{\left\{ \int_{\mathcal{V}} d\mathbf{r} [\nabla q_{\text{im}}^{(1)}(\mathbf{r})]^2 \times \int_{\mathcal{V}} d\mathbf{r} [\nabla q_{\text{im}}^{(2)}(\mathbf{r})]^2 \right\}^{1/2}}. \quad (9)$$

We calculated numerically γ_{model} as a function of the distance $2z$ between the sphere centers for different shapes of region \mathcal{V} . These different cases and the results of calculations are presented in Fig. 5(b), and we attempt to compare the result with the experimental data. It is seen that the distribution of fluctuators in thin ($\sim 0.1a$) layers that surround the spheres either completely (dotted curve) or only around equators (dashed-dotted curve) results in a rather large correlation $0.35 < \gamma_{\text{model}} < 0.75$ for the appropriate values of the distance-to-radius ratio, $1.25 < z/a < 2.5$. Such a strong correlation results from the fact that, due to the rapid ($\propto r^{-4}$) decay of polarization with distance, the product of charges induced in each sphere is maximum when a dipole is close to one of the bodies. In contrast to this, the distribution of fluctuators in the whole space (solid curve) or outside the cylinder $\rho = (r^2 - z^2)^{1/2} = a$ (that is closer to the mutual arrangement of the islands and the substrate in the real sample, dashed curve) furnishes smaller values of $\gamma_{\text{model}} \approx 0.13 - 0.22$ (in the latter case). These values are very close to those that have been measured for the present sample, Eq. (6).

IV. DISCUSSION

Using the simple model of the two-island system we have shown that the observed noise correlation ($\gamma \approx 0.1-0.2$) and, hence, noise itself can be explained by the random arrangement of *noise sources in the bulk substrate* (hypothesis 1). In the present sample, the 100-nm-wide islands lie on the Al_2O_3 layer, 200 nm thick, covering the Si foundation, hence in our case we associate noise with that layer. On the other hand, we do not preclude that the observed level of γ could be due to the combined action of fluctuators both in the tunnel barriers and the substrate. Since the sources in barriers give nearly zero correlation (due to the screening effect), those in substrate should have a correlation exceeding the 10–20 % level. According to our calculations, such a situation may occur if *the sources are located in thin layers adjacent to the islands including the barriers* (hypothesis 2). Thus the problem of determining the location of the traps is dramatized because these two hypotheses are mutually exclusive. This is, of course, true to the extent to which our assumption of the dipole character of fluctuators is valid and the model geometry is well suited to describe the sample. Since the real geometry has not been computed yet, we restrict ourselves to the following note. The numerous calculations of the integrals in Eq. (9) have shown that all reasonable modifications of the integration area give nearly the same result for γ only if this area remains part of either three-dimensional space or a thin layer surrounding the bodies. We therefore believe that our model is a reasonable approach.

In our experiment we were unable to identify the individual fluctuation sources because they are numerous and spatially distributed in an unknown way; a steady telegraph noise with a well-resolved switching between several states was not observed in the present sample. An exception was the incremental charging stimulated by the large-scale sweep of the gate voltage (see Fig. 3). These jumps of a background charge were correlated and this sustains the hypothesis 1, i.e., the noise originates in the substrate.

As to the possible tunnel barrier noise, we agree with Song *et al.*⁸ in that a SET electrometer is much more sensi-

tive to a very short displacement of the charge inside the thin ($d \sim 1-2$ nm) barrier than to that inside the substrate. Moreover, it is a matter of fact that fluctuating traps in a barrier manifest themselves in relatively large single tunnel junctions.¹¹ However, there is a radical difference between a (large) junction with a large self-capacitance and a small-capacitance junction of a SET device. When the bias current I is fixed then, in the former case, the electric field \mathbf{E} inside the barrier is maintained constant in time, while, in the latter case, the field is alternating due to sequential charging and discharging of the island by single electrons. The characteristic rate of field switching is about I/e (GHz) $\approx 6.25 \times I$ (nA) and the span $|\Delta \mathbf{E}| \epsilon d$ (mV) $\sim 0.16/C_\Sigma$ (fF). Hence, it is hard to imagine a trap under such conditions, which produces a steady telegraph signal of much smaller amplitude because in every cycle the field shakes up such a trap essentially. On the other hand, the smaller ac electric field penetrating into the substrate could activate there the frozen traps and enhance the total noise. Such an effect could in principle be observable if the second electrometer was positioned closer to the island and its charge-to-voltage response function η was large enough.

Finally, we conclude that, using the dual spectrum method, we have detected for certain that part of the background charge noise which comes from the substrate. Relying on the simple model for the two-island system we conclude that, for the present sample, a noise in the Al_2O_3 layer of the substrate most probably dominates over that of the barriers.

ACKNOWLEDGMENTS

We are pleased to thank D. E. Presnov for assistance with the sample fabrication, U. Becker for technical support in the experiment, and J. Petterson, and M. Rahman for useful comments. The work was supported by the EU (Esprit Basic Research Project 9005, Single Electronics - SETTRON), the German BMBF (Grant No. 13N6260), the Russian Program “Physics of Solid State Nanostructures” (Grant No. 1-033) and the Russian Fund for Fundamental Research (Grant No. 93-02-14136).

¹Single Charge Tunneling, Coulomb Blockade Phenomena in Nanostructures, edited by H. Grabert and M. H. Devoret (Plenum, New York, 1992).

²L. S. Kuzmin, P. Delsing, T. Claeson, and K. K. Likharev, Phys. Rev. Lett. **62**, 2539 (1989).

³L. J. Geerligs, V. F. Anderegg, and J. E. Mooij, Physica B **165**, 973 (1990).

⁴G. Zimmerli, T. M. Eiles, R. L. Kautz, and J. M. Martinis, Appl. Phys. Lett. **61**, 237 (1992).

⁵G. Zimmerli, R. L. Kautz, and J. M. Martinis, Appl. Phys. Lett. **61**, 2616 (1992).

⁶E. H. Visscher, S. M. Verbrugh, J. Lindeman, P. Hadley, and J. E. Mooij, Appl. Phys. Lett. **66**, 305 (1995).

⁷S. M. Verbrugh, M. L. Benhamadi, E. H. Visscher, and J. E. Mooij, J. Appl. Phys. **78**, 2830 (1995).

⁸D. Song, A. Amar, C. J. Lobb, and F. C. Wellstood, IEEE Trans. Appl. Supercond. **5**, 3085 (1995).

⁹J. M. Martinis, M. Nahum, and H. D. Jensen, Phys. Rev. Lett. **72**,

904 (1994).

¹⁰J. P. Pekola, A. B. Zorin, and M. A. Paalanen, Phys. Rev. B **50**, 11 255 (1994).

¹¹C. T. Rogers, R. A. Buhrman, W. J. Gallagher, S. I. Raider, A. W. Kleinsasser, and R. L. Sandstrom, IEEE Trans. Magn. **23**, 1658 (1987).

¹²See, e.g., N. F. Hooge, IEEE Trans. Electron. Dev. **41**, 1926 (1994).

¹³V. A. Krupenin, S. V. Lotkhov, and D. E. Presnov, in Nanostructures: Physics and Technology. Abstracts of Invited Lectures and Contributed Papers (Russian Academy of Sciences, St. Petersburg, 1995), pp. 354–356.

¹⁴A. B. Zorin, Rev. Sci. Instrum. **66**, 4296 (1995).

¹⁵J. S. Bendat and A. G. Piersol, Engineering Applications of Correlation and Spectral Analysis (Wiley, New York, 1980), Chap. 3.

¹⁶J. D. Jackson, Classical Electrodynamics (Wiley, New York, 1965), p. 28.